JOC Article

Effect of Ring Strain on the Thiolate−Disulfide Exchange. A Computational Study

Steven M. Bachrach,*,† Joshua T. Woody,† and Debbie C. Mulhearn‡,§

Department of Chemistry, Trinity University, 715 Stadium Drive, San Antonio, Texas 78212, and Department of Chemistry and Biochemistry, Northern Illinois University, DeKalb, Illinois 60115

sbachrach@trinity.edu

Received July 22, 2002

B3LYP/aug-cc-pVDZ and MP2/6-31+G* calculations of the reactions of HS^- with small cyclic disulfides (dithiirane, 1,2-dithietane, 1,2-dithiolane, and 1,2-dithiane) were performed to determine the reaction mechanism. For the five- and six-membered rings, the reaction proceeds via the addition−elimination pathway, consistent with acyclic analogues. The smaller, more strained three- and four-membered rings react by the S_N2 mechanism. Addition of the nucleophile cannot be accommodated by the small rings without concomitant ring cleavage.

Introduction

The thiolate−disulfide exchange provides for reversible creation and disruption of the S−S bond, of critical importance in many biological processes. While numerous solution-phase studies have implicated a simple S_N2 process for this reaction,[1−8] we have recently reported computations that suggest that the mechanism is addition−elimination in the gas phase.[9−11]

Singh and Whitesides[8] reported that 1,2-dithiolane (the cyclic five-membered disulfide) undergoes the thiolate−disulfide exchange about 600 times faster than 1,2-dithiane (the cyclic six-membered disulfide). Relief of the greater strain energy of the smaller ring results in its faster rate is suggested. They speculate that this rate enhancement is the cause for the selection of lipoic acid as a cofactor in enzymes such as the pyruvate dehydrogenase multienzyme complex.[12] Lipoic acid (as a lipoamide) serves two functions within this multienzyme, both of which involve nucleophilic substitution at sulfur: nucleophilic attack of the hydroxyethyl-TPP carbanion on the lipoamide to form acetyldihydrolipoamide-E_2 and transfer of the acetylate moiety between enzyme subunits.[13] LeMaster and Kushlan[14] have argued that compression of the angle about sulfur in the cyclic five-membered disulfide ring of thioredoxin, which mimics the angle in the presumed S_N2 transition state, leads to the high activity of this enzyme.

Gronert and Lee[15,16] have argued that formation of small, strained rings such as thiirane and oxirane proceed through relatively strain-free transition states. For example, in the reaction of $HSCH_2CH_2S^-$ to thiirane, the barrier is 19.2 kcal mol^{-1}, but the S_N2 reaction of MeS^- with ethyl sulfide has a barrier of 25.0 kcal mol^{-1}. They argue that strain energy is gained after the transition state in the formation of the small ring. In addition, to understand the energetics, one must account for 1,3-interactions and a proximity effect that favorably arranges the nucleophile near the reactive center. This leads to a much greater barrier, for example, in the formation of thietane (the four-membered ring) than thiirane (the three-membered ring), where one fewer 1,3-interactions are lost and a less favorable proximity effect is exhibited.

In this paper, we examine nucleophilic attack at sulfur in a series of cyclic disulfides, reactions 1−4 shown in Scheme 1, focusing on the effect of ring strain on the reaction mechanism. Given the computational dependencies we have previously noted for the thiolate−disulfide exchange, we examine these reactions at the B3LYP and MP2 levels.[9,11] Reactions 3 and 4, involving relatively strain-free disulfides, proceed via the expected addition−elimination route just as their acyclic analogues. On the

† Trinity University.
‡ Northern Illinois University.
§ Current address: Center for Pharmaceutical Biotechnology, University of Illinois at Chicago.

(1) Whitesides, G. M.; Lilburn, J. E.; Szajewski, R. P. *J. Org. Chem.* **1977**, *42*, 332.
(2) Wilson, J. M.; Bayer, R. J.; Hupe, D. J. *J. Am. Chem. Soc.* **1977**, *99*, 7922−7926.
(3) Freter, R.; Pohl, E. R.; Hupe, D. J. *J. Org. Chem.* **1979**, *44*, 1771−1774.
(4) Szajewski, R. P.; Whitesides, G. M. *J. Am. Chem. Soc.* **1980**, *102*, 2011.
(5) Whitesides, G. M.; Houk, J.; Patterson, M. A. K. *J. Org. Chem.* **1983**, *48*, 112−115.
(6) Hupe, D. J.; Pohl, E. R. *Isr. J. Chem.* **1985**, *26*, 395−399.
(7) Singh, R.; Whitesides, G. M. *J. Am. Chem. Soc.* **1990**, *112*, 1190−1197.
(8) Singh, R.; Whitesides, G. M. *J. Am. Chem. Soc.* **1990**, *112*, 6304−6309.
(9) Bachrach, S. M.; Mulhearn, D. C. *J. Phys. Chem.* **1996**, *100*, 3535−3540.
(10) Mulhearn, D. C.; Bachrach, S. M. *J. Am. Chem. Soc.* **1996**, *118*, 9415−9421.
(11) Bachrach, S. M.; Hayes, J. M.; Dao, T.; Mynar, J. L. *Theor. Chem. Acc.* **2002**, *107*, 266−271.
(12) Reed, L. J. *Acc. Chem. Res.* **1974**, *7*, 40−46.
(13) Voet, D.; Voet, J. G. *Biochemistry*, 2nd ed.; J. Wiley: New York, 1995.
(14) LeMaster, D. M.; Kushlan, D. M. *J. Am. Chem. Soc.* **1996**, *118*, 9255−9264.
(15) Gronert, S.; Lee, J. M. *J. Org. Chem.* **1995**, *60*, 4488−4497.
(16) Gronert, S.; Lee, J. M. *J. Org. Chem.* **1995**, *60*, 6731−6736.

10.1021/jo026223k CCC: $22.00
Published on Web 11/19/2002

SCHEME 1

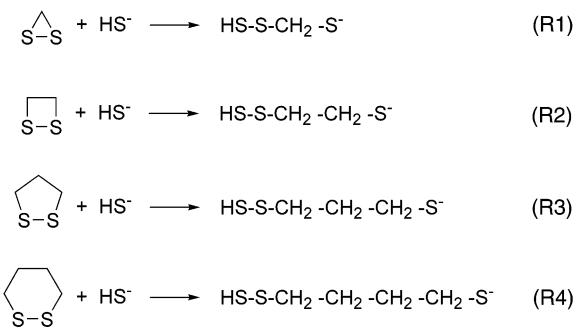

other hand, reactions 1 and 2, involving strained disulfides, proceed by the S_N2 pathway.

Computational Methods

Early studies of the thiolate−disulfide exchange noted that the HF potential energy surface (PES) consists of an entrance and exit ion−dipole complex, and a transition state connecting these two stable structures, consistent with a gas-phase S_N2 mechanism.[9,17] The PES at both MP2 and B3LYP is topologically quite different, implying a different reaction mechanism.[9,11] In addition to the two ion−dipole complexes, a third stable structure is found corresponding to the addition of the nucleophile (thiolate) to sulfur. Transition states connecting each ion−dipole to this intermediate complete the PES, which is indicative of an addition−elimination (AE) pathway. Anticipating that similar mechanism dependence is likely for reactions 1−4, we have employed the MP2/6-31+G* and B3LYP/aug-cc-pVDZ methods.[18,19] These methods differ in their treatment of electron correlation and allow for comparison of the methods in terms of the nature of the PES. Previous calculations have shown the PES and reaction energetics for thiolate−acyclic disulfide exchange are very similar for these two computational methods.[11] Furthermore, a recent exhaustive comparison of DFT methods to CCSD applied to S_N2 reactions at carbon indicate that B3LYP provides reasonable geometries and energies; important systematic deficiencies of B3LYP are overestimation of the hydrogen bond distance in ion−dipole complexes and underestimation of the ion−dipole complex energy and activation barrier.[20]

A cautionary note needs be mentioned here with regard to the relative energies of critical points along the reaction pathways. The Schaefer et al.[20] DFT study cautions that B3LYP activation barriers for S_N2 reactions are likely underestimated by 2 kcal mol^{-1}. Some of the barriers obtained in this study are on this order or less—and for the two reactions that *are* S_N2 reactions (reactions 1 and 2), the B3LYP and MP2 barriers are within 2 kcal mol^{-1}. It is important to recognize that the goal of this study is the nature of the potential energy surface and, because of the difficulty in accurately determining barriers, the energetics are of secondary importance. For all of the nucleophilic substitution reactions at sulfur we have examined, both in this study and previously, MP2 and B3LYP provide identical topologies for the PES. The only exception is the lack of intermediates or transition states for the chair conformation for reaction 4 at MP2, despite exhaustive searches. We therefore believe that the computational methods employed here are suitable for our purpose of explicating the PES, and thus the mechanism of nucleophilic substitution at sulfur in strained rings.

We attempted to locate entrance ion−dipole complexes, transition states, and intermediates for reactions 1−4 by complete geometry optimization at both MP2/6-31+G* and B3LYP/aug-cc-pVDZ. Multiple conformations of the rings, especially for the five- and six-membered rings, were explored in the searches for transition states and intermediates. We report only those transition states that correspond to substitution reactions. There are multiple local minima that correspond to different conformations of the products; we report only the conformation directly connected to the transition state. The nature of all structures was confirmed using analytical frequencies; all reactants, ion−dipole complexes, intermediates, and products had only positive eigenvalues of the Hessian matrix, while all transition states had one and only one negative eigenvalue of the Hessian matrix. The optimized B3LYP structures are shown in Figures 1−7, and relevant distances (for both the B3LYP and MP2 structures) are listed in Table 1. Throughout the paper, we refer to the incoming sulfur as S_{nuc} and the exiting sulfur as S_{lg}. We employ the following labeling scheme: for all cases, ***n*** designates the reaction number, and we designate reactants as **R-*n***, ion−dipole complexes as **ID-*n***, entrance transition states as **TS1-*n***, intermediates as **INT-*n***, exit transition states as **TS2-*n***, products as **P-*n***, and proton-transfer products as **PTP-*n***. All energies include the electronic energy and the zero-point vibrational energies, scaled by 0.96 and 0.98 for the MP2 and the B3LYP results, respectively. All computations were performed with GAUSSIAN-98.[21]

Results

Geometries and Ring Strain Energies of R-1−R-4. The structures of the cyclic disulfides are shown in Figure 1; both the chair and boat forms of **R-4** were located. These geometries are as expected. The MP2 S−S and S−C distances are all shorter than the B3LYP distances (see Table 1), but the difference is very small.

Ring strain energy (RSE) is determined using the group equivalent approach.[22] RSEs are evaluated as the negative of the reaction energy for eq 1. These RSEs are

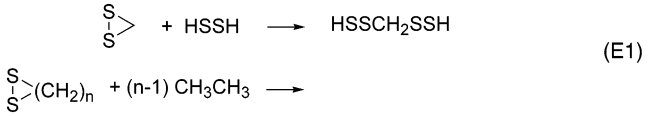

(E1)

given in Table 2. The MP2 and B3LYP estimates are in good general agreement, and one can therefore anticipate that these two methods should conform with each other when applied to the reactions under study. Calorimetric estimation[23] of the RSE of **R-3** and **R-4** is 4 and 0.5 kcal mol^{-1}, respectively. These agree with the calculated RSEs of about 6 kcal mol^{-1} for **R-3** and 2 kcal mol^{-1} for **R-4**. The smaller rings are significantly more strained: the RSE of **R-1** is about 19 kcal mol^{-1}, and that for **R-2** is

(17) Aida, M.; Nagata, C. *Chem. Phys. Lett.* **1984**, *112*, 129−132.
(18) Becke, A. D. *J. Chem. Phys.* **1993**, *98*, 5648−5650.
(19) Dunning, T. H. J. *J. Chem. Phys.* **1989**, *90*, 1007−1023.
(20) Gonzales, J. M.; Cox, S. C. I.; Brown, S. T.; Allen, W. D.; Schaefer, H. F. I. *J. Phys. Chem. A* **2001**, *105*, 11327−11346.
(21) Frisch, M. J.; Trucks, G. W.; Schlegel, H. B.; Scuseria, G. E.; Robb, M. A.; Cheeseman, J. R.; Zakrzewski, V. G.; Montgomery, J. A. J.; Stratmann, R. E.; Burant, J. C.; Dapprich, S.; Millam, J. M.; Daniels, A. D.; Kudin, K. N.; Strain, M. C.; Farkas, O.; Tomasi, J.; Barone, V.; Cossi, M.; Cammi, R.; Mennucci, B.; Pomelli, C.; Adamo, C.; Clifford, S.; Ochterski, J.; Petersson, G. A.; Ayala, P. Y.; Cui, Q.; Morokuma, K.; Malick, D. K.; Rabuck, A. D.; Raghavachari, K.; Foresman, J. B.; Cioslowski, J.; Ortiz, J. V.; Baboul, A. G.; Stefanov, B. B.; Liu, G.; Liashenko, A.; Piskorz, P.; Komaromi, I.; Gomperts, R.; Martin, R. L.; Fox, D. J.; Keith, T.; Al-Laham, M. A.; Peng, C. Y.; Nanayakkara, A.; Gonzalez, C.; Challacombe, M.; Gill, P. M. W.; Johnson, B.; Chen, W.; Wong, M. W.; Andres, J. L.; Gonzalez, C.; Head-Gordon, M.; Replogle, E. S.; Pople, J. A. *GAUSSIAN-98*; A.7 ed.; Gaussian, Inc.: Pittsburgh, PA, 1998.
(22) Bachrach, S. M. *J. Chem. Educ.* **1990**, *67*, 907−908.
(23) Sunner, S. *Nature* **1955**, *176*, 217.

TABLE 1. Selected Geometric Parameters of Critical Points in Reactions 1−4[a]

Reactants

	S−S_{lg}			S−S_{lg}			S−S_{lg}	
compound	MP2	B3LYP	compound	MP2	B3LYP	compound	MP2	B3LYP
R-1	2.104	2.132	**R-3**	2.075	2.114	**R-4boat**	2.061	2.099
R-2	2.132	2.170	**R-4**	2.067	2.107			

Ion−Dipole Complexes

	S−S_{lg}		S_{nuc}···H	
compound	MP2	B3LYP	MP2	B3LYP
ID-1	2.107	2.133	2.459	2.476
ID-2	2.127	2.163	2.996	3.030
			2.958	3.003
ID-3	2.121	2.159	2.784	2.730
ID-4	2.071	2.112	2.691	2.620

Transition State 1

	S−S_{lg}		S_{nuc}···H		S_{nuc}··· S		S_{nuc}–S S_{lg}	
compound	MP2	B3LYP	MP2	B3LYP	MP2	B3LYP	MP2	B3LYP
TS11	2.120	2.151	2.880	2.855	3.826	4.191	111.7	105.8
TS12	2.150	2.196	2.531	2.525	3.933	4.294	137.7	128.5
TS13	2.116	2.156	2.648	2.543	3.298	3.850	165.9	155.2
TS14chair		2.135		2.548		3.847		164.1
TS14boat	2.123	2.256	2.733	2.755	3.254	2.916	178.5	174.6

Intermediate

	S−S_{lg}		S_{nuc}−S		S_{nuc}−S S_{lg}	
compound	MP2	B3LYP	MP2	B3LYP	MP2	B3LYP
INT-3	2.442	2.502	2.524	2.552	177.3	179.0
INT-4chair		2.295		2.810		177.7
INT-4boat	2.417	2.593	2.536	2.454	178.5	179.3

Transition State 2

	S···S_{lg}		S_{nuc}−S		S_{nuc}−S S_{lg}	
compound	MP2	B3LYP	MP2	B3LYP	MP2	B3LYP
TS22		4.111		2.115		118.2
TS23	3.765	3.967	2.081	2.129	145.6	144.0
TS24chair		3.824		2.139		159.8
TS24boat	3.895	3.895	2.096	2.144	171.4	163.7

Product

	S_{nuc}−S			S_{nuc}−S			S_{nuc}−S	
compound	MP2	B3LYP	compound	MP2	B3LYP	compound	MP2	B3LYP
P-1	2.121	2.237	**P-2a**		2.115	**P-4**	2.071	2.108
P-2	2.121	2.308	**P-3**	2.074	2.124			

[a] All distances in angstroms and all angles in degrees.

even higher, about 22 kcal mol^{-1}. These can be compared to the RSEs of the small rings containing a single sulfur: thiirane, 19.1 kcal mol^{-1}; thietane, 22.2 kcal mol^{-1}; tetrahydrothiophene, 3.1 kcal mol^{-1}.[1]

Geometries. Thiolate and any disulfide will associate to form an ion−dipole complex in the gas phase. This is well established in both experiments and computations. As noted by Gronert[15,16] for ion−dipole complexes of thiirane and oxirane, with larger disulfides a number of configurations of the ion−dipole complex are possible with little energy difference among them. We have not performed an exhaustive search of the ion−dipole space, figuring that any ion−dipole structure is likely to not be significantly higher in energy than the actual minimum energy complex, if the structure we found is not actually the optimum structure. Thus, one can consider the structures shown in Figure 2 as representative of the ion−dipole space. Formation of the complex barely perturbs the cyclic disulfide geometry (see Table 1 for the S−S distances). The putative hydrogen bond distance is little affected by the computational method. This distance is longer in **ID-2** than the others due to the bridging position of thiolate. (Repeated attempts failed to locate an ion−dipole structure for reaction 2 that does not involve a bridging thiolate ion.)

The reaction proceeds from the ion−dipole complex with the thiolate swinging toward the disulfide bond, thereby lengthening the putative hydrogen bond of the ion−dipole complex. These transition states are shown in Figure 3 , and important distances are listed in Table 1. At B3LYP, we located two TSs for reaction 4, corresponding to attack of the boat and chair form of the six-membered ring, while at MP2 only the boat form was found. The S−S_{lg} distance is only slightly longer in these

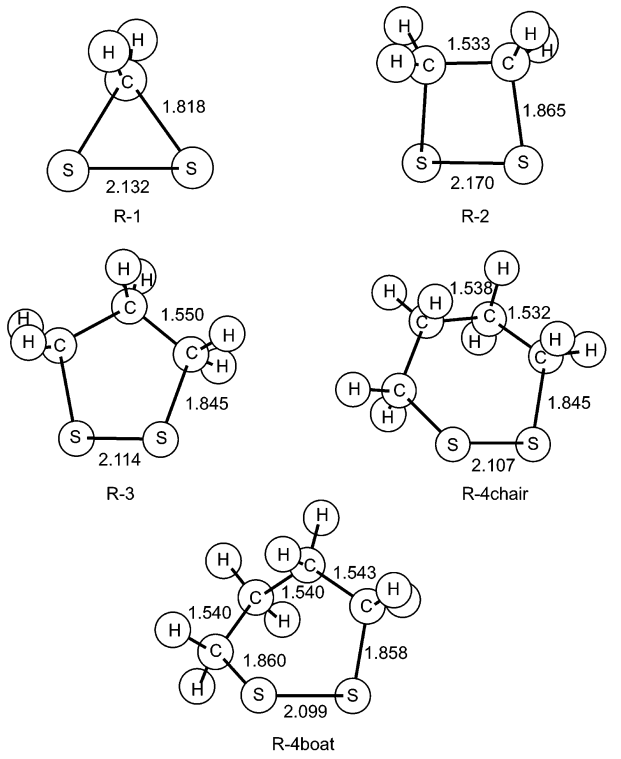

FIGURE 1. B3LYP/aug-cc-pVDZ-optimized geometries of **R-1**−**R-4**. All distances are in angstroms, and all angles are in degrees.

TABLE 2. Ring Strain Energy (kcal mol^{-1}) from Eq 1

compound	B3LYP	MP2	compound	B3LYP	MP2
R-1	18.7	20.5	**R-4chair**	2.0	1.6
R-2	20.8	23.9	**R-4boat**	6.6	6.7
R-3	5.8	6.4			

TSs than in the reactants, and the $S_{nuc}\cdots S$ distance is very long. The $S_{nuc}\cdots S\cdots S_{lg}$ angle is decidedly nonlinear. Clearly, these are early TSs with an attack angle that is inconsistent with backside linear attack found in the classic S_N2 mechanism. The B3LYP and MP2 geometries are reasonably similar: the MP2 $S-S_{lg}$ distance is only slightly shorter than at B3LYP, and only for **TS1-3** is the $S_{nuc}\cdots H$ distance different by more than 0.1 Å. There is greater discrepancy in the $S_{nuc}\cdots S$ distances. MP2 predicts a much closer approach of the nucleophile than B3LYP, except in **TS-4boat**. The geometry of **TS-4chair** indicates a much earlier transition state than **TS4-boat**; its $S-S_{lg}$ distance is shorter, the $S_{nuc}-S$ distance is much longer, and the $S_{nuc}-S-S_{lg}$ angle is much narrower than in the boat form.

There is a divergence in the reaction pathway forward from **TS1**: reactions 3 and 4 proceed through an intermediate (**INT-3** and **INT-4**), while no intermediate is found for reactions 1 and 2 (**TS1-1** connects directly to **P-1**, and **TS1-2** connects directly to **P-2**). The intermediates are drawn in Figure 4, and important distances are listed in Table 1.

INT-3 and **INT-4boat** are representative of typical intermediates we have seen in our previous studies of nucleophilic substitution at S; the two S−S bonds are of similar length and in the vicinity of 2.5 Å, and the S−S−S angle is nearly linear. Like **INT-4boat**, **INT4-chair** has

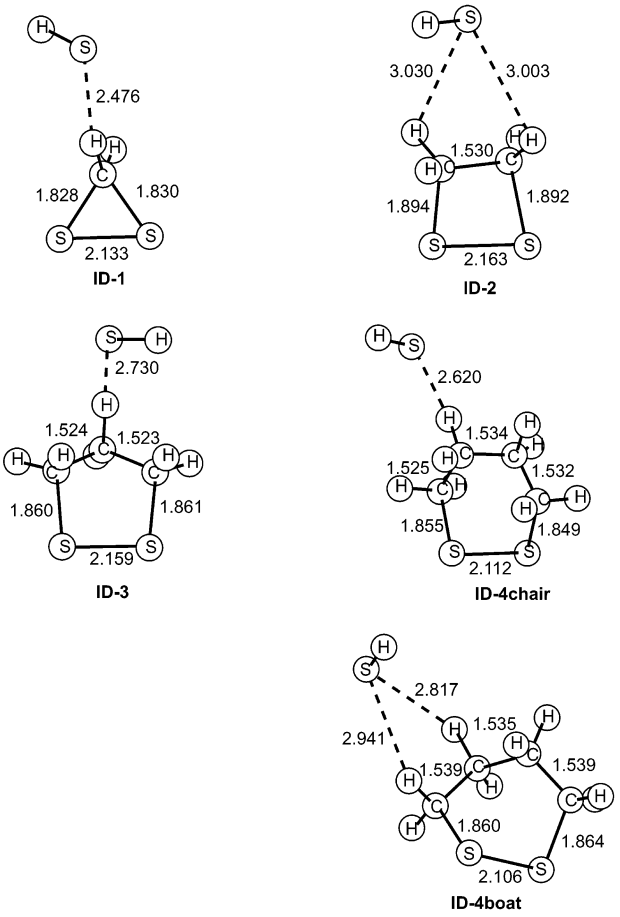

FIGURE 2. B3LYP/aug-cc-pVDZ-optimized geometries of **ID-1**−**ID-4**. See Figure 1.

a nearly linear S−S−S angle, but the S−S distances are quite different. The $S_{nuc}\cdots S$ distance is very long (2.810 Å), though this is much shorter than in **TS1-4chair**. The $S-S_{lg}$ bond has lengthened by 0.16 Å from that in **TS1-4chair**, but remains much shorter than typical distances in intermediates we have previously encountered. Besides the differences in the S−S distances, the two intermediates from reaction 4 differ in the conformation about the ring, one in a boatlike form and the other in a chairlike form. As for **TS1-4**, only a boat form of the intermediate for reaction 4 (**INT-4boat**) is found at MP2. The two MP2 intermediates (**INT-3** and **INT-4boat**) are structurally similar to their B3LYP complements, though the asymmetry in the lengths of the two S−S interactions is somewhat larger at MP2.

Continuing on for reactions 3 and 4, after the intermediate is a second transition state, **TS2-3** and **TS2-4**. These second TSs are drawn in Figure 5, and important distances are listed in Table 1. In these TSs, the $S-S_{nuc}$ bond is fully formed and the $S-S_{lg}$ bond very long, about 4 Å. There is little difference between the B3LYP and MP2 geometries. These TSs mostly involve the opening up of the ring by rotations about the C−C bonds.

The direct products of reactions 1−4 are drawn in Figure 6 and some of their bond distances listed in Table 1. A comprehensive search for the lowest energy conformation of the products was not performed, and these are simply representative of the product space. As for the

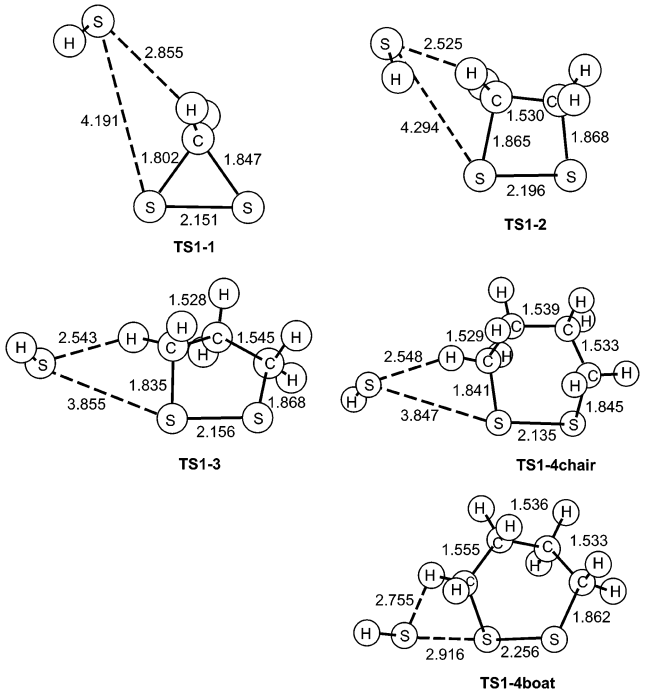

FIGURE 3. B3LYP/aug-cc-pVDZ-optimized geometries of **TS1**−**1**−**TS1**−**4**. See Figure 1.

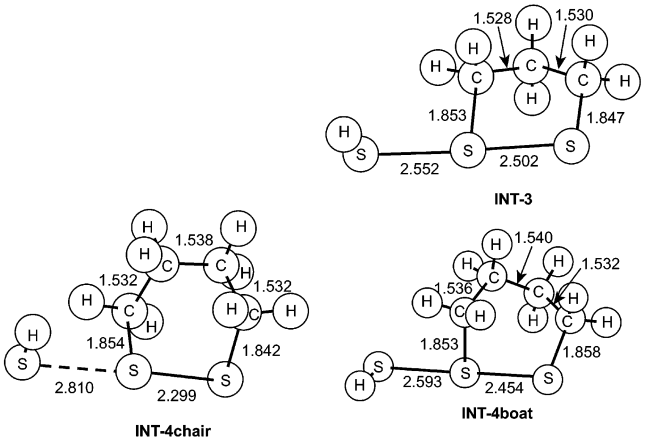

FIGURE 4. B3LYP/aug-cc-pVDZ-optimized geometries of **INT-3**−**INT-4**. See Figure 1.

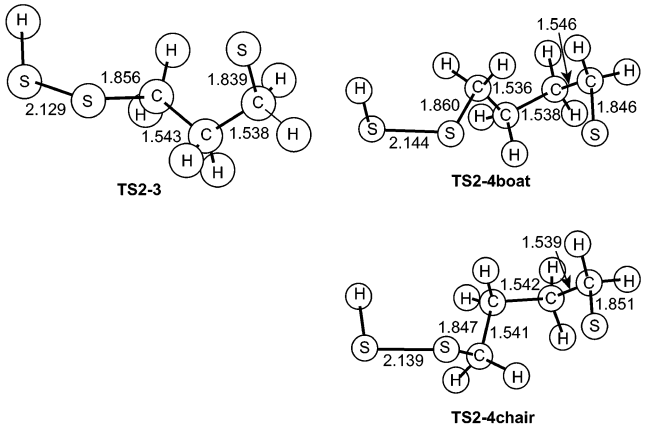

FIGURE 5. B3LYP/aug-cc-pVDZ-optimized geometries of **TS2-3**−**TS2-4**. See Figure 1.

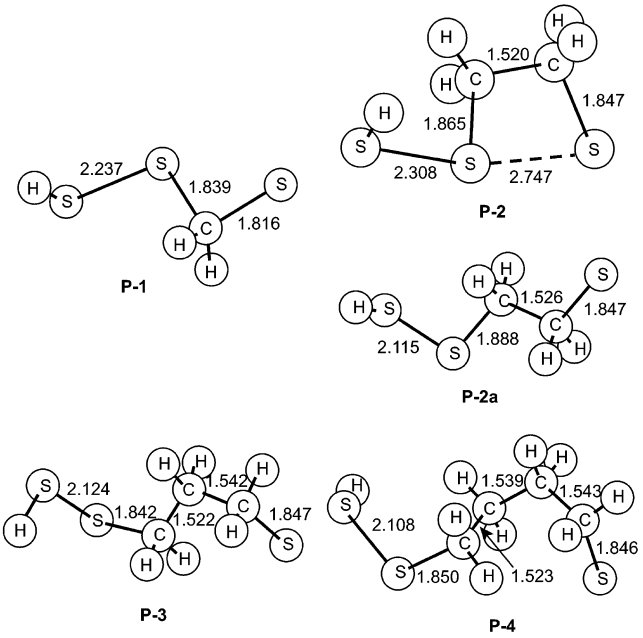

FIGURE 6. B3LYP/aug-cc-pVDZ-optimized geometries of **P-1**−**P-4**. See Figure 1.

cyclic reactants, the structures of **P-1**, **P-3**, and **P-4** are quite normal and expected. MP2 S−S distances are again slightly shorter than the B3LYP values.

P-2 obtained at MP2 is also ordinary, with a normal S_{nuc}−S distance and a long, broken S−S_{lg} distance. However, the B3LYP product of reaction 2 is rather unusual: the S−S_{nuc} distance (2.308 Å) is much longer than a typical S−S bond, and the S−S_{lg} distance (2.747 Å) is short enough to suggest some possible remaining interaction. It is tempting to identify this structure as an intermediate. We did locate a transition state leading from this structure to a structure with a completely broken S−S_{lg} bond (**P-2a**). Motion along the imaginary frequency in this transition state corresponds primarily to rotation about the C−C bond, suggesting that **P-2** and **P-2a** are simply conformers. Further, **P-2** is much more stable than the intermediates found in reactions 3 and 4 or in our previous studies. It is energetically much more in line with the product of reaction 1.

All attempts to locate a cyclic product having an intramolecular hydrogen bond between the disulfide hydrogen and the sulfur anion led to proton transfer. The proton from the terminus of the disulfide transfers to the sulfur anion, creating a more stable disulfide anion. These products, referred to as **PTP-1**−**PTP-4** for proton-transfer product, are cyclic, having an intramolecular hydrogen bond between the thiol and disulfide anion. They are drawn in Figure 7. Again, these structures are as expected, and there are only minor differences between the B3LYP and MP2 structures.

Energetics.The relative energies of all structures in reactions 1−4 are listed in Table 3. We will first examine the energetics of each reaction individually and then compare them.

Formation of the ion−dipole complex is exothermic by about 11 kcal mol^{-1} in reaction 1. The complex is predicted to be about 1 kcal mol^{-1} more stable at MP2

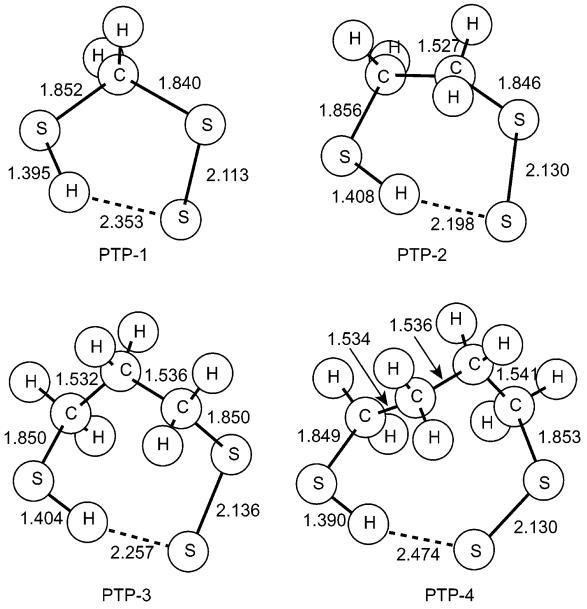

FIGURE 7. B3LYP/aug-cc-pVDZ-optimized geometries of **PTP-1**−**PTP-4**. See Figure 1.

TABLE 3. Relative Energies (kcal mol^{-1}) for Reactions 1−4

	R	ID	TS1	INT	TS2	P	PTP
1 B3LYP	0.0	10.4	−9.6			−28.9	−30.6
MP2	0.0	11.6	−10.3			−26.0	−32.1
2 B3LYP	0.0	12.4	−10.1			−24.0	−30.3
MP2	0.0	13.9	−10.8			−23.1	−35.2
3 B3LYP	0.0	11.5	−8.7	−12.61	−2.0	−5.7	−16.2
MP2	0.0	13.7	−9.4	−9.72	−1.8	−6.9	−18.8
4 B3LYP	0.0(C)	9.1(C)	−8.1(C)	−9.41(C)	−3.2(C)	−0.2	−13.3
MP2	4.6(B)	5.4(B)	−3.7(B)	−5.72(B)	−2.3(B)	−2.3	−16.8
	0.0(C)	11.5(C)	−0.6(B)	−3.22(B)	−4.6(B)		
	5.1(B)	7.4(B)					

and B3LYP. The reaction barrier is then computed relative to this ion−dipole; it is 0.8 kcal mol^{-1} at B3LYP and 1.24 kcal mol^{-1} at MP2—both very small values, and this TS lies well below the reactant energies. This TS directly connects to the product **P-1**; at B3LYP, it lies 28.9 kcal mol^{-1} below the reactants, 18.5 kcal mol^{-1} below **ID-1**, and 19.4 kcal mol^{-1} below **TS-1**. The product is slightly less stable at MP2. The proton transfer releases 1.7 kcal mol^{-1} (6.1 kcal mol^{-1} at MP2) to give the final product **PTP-1**.

At B3LYP, reaction 2 first forms an ion−dipole complex that lies 12.4 kcal mol^{-1} below the reactants. A barrier of only 2.1 kcal mol^{-1} precedes formation of **P-2**, which is 11.5 kcal mol^{-1} below **ID-2**. Proton transfer leads to **PTP-2**, which lies 7.6 kcal mol^{-1} below **P-2** or 30.3 kcal mol^{-1} below the reactants. A similarly shaped potential energy surface is found at MP2. An ion−dipole complex is formed (slightly more exothermic than at B3LYP), and then a small barrier (3.1 kcal mol^{-1}) intervenes before formation of **P-2**, which is 9.2 kcal mol^{-1} below **ID-2**. Subsequent proton transfer is very exothermic, −12.1 kcal mol^{-1}.

B3LYP and MP2 are in very close energetic agreement for all structures in reaction 3. Therefore, just describing the surface at B3LYP, **ID-3** is 11.5 kcal mol^{-1} below the reactants. The barrier to the intermediate **INT-3** is 3.9 kcal mol^{-1}, which is 1.1 kcal mol^{-1} below **ID-3**. The second barrier is 10.6 kcal mol^{-1} above **INT-3** and only 1.95 kcal mol^{-1} below the reactants. Formation of **P3** is endothermic from the intermediate (+6.9 kcal mol^{-1}), though it is 5.7 kcal mol^{-1} below the reactants. Proton transfer is 10.5 kcal mol^{-1} exothermic, giving an overall reaction energy of −16.2 kcal mol^{-1}.

In principle, reaction 4 can proceed via reaction of the chair and boat forms of **R-4**. The chair form is 4.6 kcal mol^{-1} below the boat form at B3LYP and 5.1 kcal mol^{-1} at MP2. Despite extensive search, we could not locate a chair form of either the intermediate or entrance transition state at MP2/6-31+G*, but only boat forms: **TS1-4boat** and **INT-4boat**. On the other hand, both chair and boat pathways could be identified at B3LYP/aug-cc-pVDZ. Before considering the two pathways, we can discuss the overall energetics. Production of **P-4** is at best only slightly exothermic: −0.2 kcal mol^{-1} at B3LYP and −2.3 kcal mol^{-1} at MP2. The internal proton transfer to give **PTP-4** is strongly exothermic by 13.1 kcal mol^{-1} (14.5 at MP2), and it is this that drives the overall reaction in the gas phase.

Following the boat pathway, the ion−dipole complex lies 9.9 kcal mol^{-1} below the reactant at B3LYP (12.5 kcal mol^{-1} at MP2). The barrier to the intermediate **INT-4boat** is 1.7 kcal mol^{-1} at B3LYP but much larger (6.8 kcal mol^{-1}) at MP2. While the intermediate is predicted to lie below the reactants with both computational methods, B3LYP predicts it to also lie below **ID4-boat**, while MP2 indicates that it is 4.2 kcal mol^{-1} above the ion−dipole complex. The two methods are similar in their estimate of the second barrier, 8.0 (B3LYP) and 7.8 (MP2) kcal mol^{-1}.

The chair form of the ion−dipole complex lies about 10 kcal mol^{-1} below the reactants. From here forward, the chair pathway is found only at B3LYP. Repeated attempts to locate this pathway using the MP2 method led to dissociation to reactants only, even when beginning with the B3LYP structures. From **ID-4chair**, a barrier of only 1.0 kcal mol^{-1} intercedes formation of the intermediate **INT-4chair**. This intermediate is only 0.4 kcal mol^{-1} more stable than **ID-4chair**. The next barrier is quite large, 12.6 kcal mol^{-1}.

Discussion

The main purpose of this work is to ascertain the mechanism for nucleophilic substitution at sulfur in a cyclic disulfide. Therefore, this discussion will focus on this issue.

First, we will summarize the salient points from our previous studies. For the simple prototype nucleophilic substitution reactions (reactions 5−7),

$$HS^- + HS{-}SH \rightarrow HS{-}SH + HS^- \quad \text{(R5)}$$

$$MeS^- + HS{-}SMe \rightarrow MeS{-}SH + MeS^- \quad \text{(R6)}$$

$$HS^- + MeS{-}SH \rightarrow HS{-}SMe + HS^- \quad \text{(R7)}$$

the potential energy surface at both MP2/6-31+G* and B3LYP/aug-cc-pVDZ has three wells, corresponding to entrance and exit ion−dipole complexes and an intermediate, and two transition states connecting the ion−

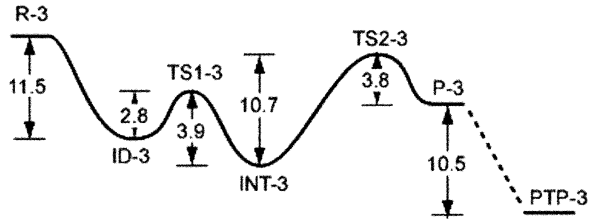

FIGURE 8. Potential energy surface for reaction 3 with relative B3LYP/aug-cc-pVDZ energies in kilocalories per mole.

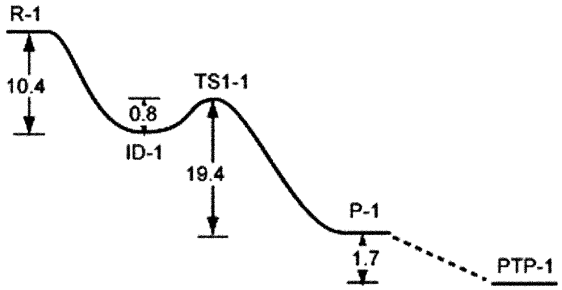

FIGURE 9. Potential energy surface for reaction 1 with relative B3LYP/aug-cc-pVDZ energies in kilocalories per mole.

dipoles to the intermediate. This surface corresponds to an addition−elimination mechanism. The depth of the intermediate well is smaller at MP2 than at B3LYP by 2−3 kcal mol^{-1}. In fact, for reaction 7, the well is quite shallow, only 0.1 kcal mol^{-1} at MP2, raising some doubt as to the nature of the mechanism (though the well depth is 2.8 kcal mol^{-1} at B3LYP). Additional steric bulk at the sulfur under attack might switch the mechanism to S_N2. On the basis of these results, we anticipated that the larger cyclic disulfides would undergo addition−elimination reactions, but perhaps with increased strain, the smaller rings might follow the S_N2 path.

Nucleophilic attack of sulfur in 1,2-dithiolane (reaction 3) or 1,2-dithiane (reaction 4) proceeds by an addition−elimination pathway. Figure 8 shows the PES for reaction 3, and topologically represents the PES for reaction 4 as well. It is characterized by three local minima: the ion−dipole complex, the intermediate, and the product. The S_N2 mechanism is incompatible with the observation of the intermediate. Since the ring strain energy of **R-3** and **R-4** is small, an intermediate containing a hypercoordinate sulfur can be accommodated, resulting in the addition−elimination mechanism.

Even though the sulfur under attack bears a carbon atom, which resulted in a very shallow intermediate well in the prototype reaction 7, the intermediates in reactions 3 and 4 sit in reasonably deep wells. The entrance into the well is shallower than the exit. **TS1-3** lies 2.8 kcal mol^{-1} at B3LYP (4.4 kcal mol^{-1} at MP2) above **INT-3**, while **TS2−3** is 10.7 kcal mol^{-1} at B3LYP (7.9 kcal mol^{-1} at MP2) above **INT-3**. Similar barrier heights exist for reaction 4, though the entrance is slightly lower in reaction 3.

Reactions 1 and 2 involving attack upon dithiirane and 1,2-dithietane, the smallest cyclic disulfides, proceed via the S_N2 mechanism. Both the B3LYP and MP2 calculations concur on this pathway, sketched in Figure 9 for reaction 1. A single transition state separates reactants from product, with no intervening intermediates. While the attack angle ($S_{nuc}-S-S_{lg}$) is not strictly 180°, reflecting the need to break the hydrogen bond in **ID-1** along with forming the new S−S bond, the form of the potential energy surface is consistent with the S_N2 mechanism.

TABLE 4. Relative Energies (kcal mol^{-1}) of Model Geometries of the Intermediate[a]

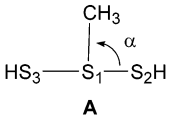

A

α (deg)	rel *E*	α (deg)	rel *E*
60	30.8	80	1.7
70	9.2	90	0.0

[a] Geometry optimized at B3LYP/6-31+G* with $r(S_1-S_2) = 2.5$ Å and α fixed to specified values.

For the thiolate−disulfide exchange, one can differentiate the S_N2 mechanism from the AE mechanism simply on one point: the S_N2 transition state vs the AE intermediate. These have similar structures; for example, the HF/6-31G* transition state for reaction 5 is nearly structurally identical to the MP2/6-31+G* intermediate.[9] Which mechanism occurs can be thought of in terms of whether this structure is stable enough to be an intermediate. For reactions 3 and 4, this structure is an intermediate, just as for the acyclic analogues. For reactions 1 and 2, this structure is not stable and is a transition state. This suggests that these have too much strain energy.

To qualitatively assess the strain in this putative "intermediate/TS" structure, we have modeled this structure as **A** shown in Table 4. We fix the S_1-S_2 distance at 2.5 Å, close to the typical distance found in the intermediates of reactions 5−7. We then optimize the structure with the further constraint of holding the $C-S_1-S_2$ angle (α) to 90°, 80°, 70°, and 60° to mimic an intermediate that has a small ring. The resulting relative energies are listed in Table 4. Clearly, as the angle about the central sulfur (S_1) contracts, the intermediate becomes less stable, with dramatic destabilization when α is less than 70°. The corresponding angle α in **R-3** and **R-4** is 91.0° and 98.5°, respectively, and so these larger rings can accommodate the incoming nucleophile and create a stable intermediate. On the other hand, α is 78.3° in **R-2** and only 54.0° in **R-1**. Addition of the nucleophile to these strained rings cannot be accommodated without simultaneous cleavage of the ring; to do otherwise would dramatically increase the strain in the system.

Gronert and Lee[15,16] have argued for "strain-free" transition states in nucleophilic substitution reaction at carbon that result in small rings. A similar type analysis is problematic here in that the mechanism for substitution upon the ring and its acyclic analogue are different. Reactions 1 and 2 proceed via the S_N2 mechanism, while the acyclic reference is reaction 5, which proceeds by addition−elimination. Their transition states are therefore not comparable in the sense employed by Gronert and Lee. However, one can compare the reaction barriers for the reverse of reactions 1 and 2 and compare these with the RSEs of **R-1** and **R-2**. The B3LYP barrier for the reverse of reaction 1 is 19.4 kcal mol^{-1} and 15.7 kcal mol^{-1} at MP2, which are near the RSE of **R-1**. On the

other hand, the reverse barrier of reaction 2, 13.9 and 12.3 kcal mol^{-1} at B3LYP and MP2, respectively, is substantially less than the RSE of **R-2**. If one considers that the intrinsic barrier to nucleophilic substitution at S is constant (and the barriers of reactions 5−7 are very similar), then the differences in these two barriers reflect the added ring strain built into the transition state. Therefore, reaction 1 certainly has substantial strain energy at its transition state, in contrast to the findings for substitution at carbon. This is not unexpected given the structure of **TS1-1**, where there is little lengthening of the S−S bond within the ring relative to that of **R-1**. Both **TS1-1** and **TS1-2** are geometrically very early, and significant loss of the RSE is thus unlikely.

Last, we comment on the relative energetics for reactions 3 and 4. Whitesides has claimed that the greater strain of the smaller five-membered ring or the six-membered ring leads to its greater rate toward nucleophilic substitution. Direct comparisons of barrier heights is complicated by the addition−elimination mechanism and the nature of gas-phase chemistry. For example, formation of **ID-3** is more exothermic than that of **ID-4**, and so judging the barrier height to the intermediate is complicated by the relative stabilities of the ion−dipole complexes. This barrier is only 1 kcal mol^{-1} for reaction 4 but 2.8 kcal mol^{-1} for reaction 3—a difference that matches the relative stabilities of the ion−dipole complexes. The second transition state is complicated in the same way: **INT-3** is more stable than **INT-4**, leading to a higher barrier from the former.

However, some clarity can be gained by examining the energies of the transition states relative to the reactants. For both reactions 3 and 4, the second transition state is predicted to be rate limiting. **TS2-3** is nearly 2 kcal mol^{-1} lower in energy than the isolated reactants, while **TS2-4** is 2−4 kcal mol^{-1} higher in energy than the reactants. This suggests that reaction 3 will be kinetically more facile than reaction 4, consistent with Whitesides' results.[8] In addition, reaction 3 is overall exothermic, while reaction 4 is essentially thermoneutral. These results add further support to Whitesides' supposition for the natural selection of lipoic acid as a cofactor.

Conclusion

The mechanism for gas-phase nucleophilic substitution at sulfur in cyclic disulfides is dependent on the size of the ring. For the very strained three- and four-membered rings, dithiirane **R-1** and 1,2-dithietane **R-2**, the reaction follows the S_N2 pathway, though the angle formed by the nucleophilic sulfur and the disulfide sulfurs is not linear. On the other hand, the larger rings, 1,2-dithiolane **R-3** and 1,2-dithiane **R-4**, are much less strained, and nucleophilic substitution upon them proceeds by the addition−elimination pathway. Addition−elimination is the pathway for nucleophilic substitution of acyclic disulfides as well. The strain energy of the small rings precludes the formation of an intermediate, thereby excluding the AE mechanism.

Acknowledgment. The support of grants from the Robert A. Welch Foundation (W-1442) and the Petroleum Research Fund, administered by the American Chemical Society, are gratefully acknowledged.

Supporting Information Available: Coordinates of all optimized B3LYP/aug-cc-pVDZ and MP2/6-31+G* structures, their absolute energies, and number of imaginary frequencies. This material is available free of charge via the Internet at http://pubs.acs.org.

JO026223K